MNRAS **435,** 3541–3546 (2013)
Advance Access publication 2013 September 9
doi:10.1093/mnras/stt1544

CN excitation and electron densities in diffuse molecular clouds

Stephen Harrison,[1]⋆ Alexandre Faure[2] and Jonathan Tennyson[1]

[1]*Department of Physics and Astronomy, University College, London, Gower Street, London WC1E 6BT, UK*
[2]*UJF-Grenoble 1/CNRS-INSU, Institut de Planétologie et d'Astrophysique de Grenoble (IPAG) UMR 5274, Grenoble, F-38041, France*

Accepted 2013 August 14. Received 2013 August 13; in original form 2013 July 3

ABSTRACT

Utilizing previous work by the authors on the spin-coupled rotational cross-sections for electron–CN collisions, data for the associated rate coefficients are presented. Data on rotational, fine-structure and hyperfine-structure transition involving rotational levels up to $N = 20$ are computed for temperatures in the range 10–1000 K. Rates are calculated by combining Born-corrected R-matrix calculations with the infinite-order-sudden approximation. The dominant hyperfine transitions are those with $\Delta N = \Delta j = \Delta F = 1$. For dipole-allowed transitions, electron-impact rates are shown to exceed those for excitation of CN by para-$H_2(j = 0)$ by five orders of magnitude. The role of electron collisions in the excitation of CN in diffuse clouds, where local excitation competes with the cosmic microwave background photons, is considered. Radiative transfer calculations are performed and the results compared to observations. These comparisons suggest that electron density lies in the range $n(e) \sim 0.01$–$0.06\,\mathrm{cm}^{-3}$ for typical physical conditions present in diffuse clouds.

Key words: astrochemistry – molecular data – molecular processes – scattering – ISM: abundances – ISM: molecules.

1 INTRODUCTION

Soon after its discovery by Penzias & Wilson (1965), the cosmic microwave background (CMB) was postulated as primarily responsible for the rotational excitation of CN observed in diffuse clouds (Field & Hitchcock 1966; Thaddeus & Clauser 1966). Optical absorption-line measurements of interstellar CN have thus long been used to estimate the temperature of CMB radiation at 2.6 and 1.3 mm, the wavelengths of the two lowest CN rotational transitions (Thaddeus 1972). It was soon realized, however, that the accuracy of this indirect method is limited by line saturation and local collisional excitation effects. Since the first high accuracy measurements of the CMB temperature by the *COBE* satellite (Mather 1990), with the latest value at $T_{\mathrm{CMB}} = 2.72548 \pm 0.00057$ K (Fixsen 2009), CN absorption line observations have been used to provide an independent calibration of the *COBE* satellite, to sample the CMB far from the near-Earth environment, and to measure the rotational excitation of CN in excess of T_{CMB}, i.e. the local excitation processes. Differences between the *COBE* results and those from CN have recently been discussed by Leach (2012).

CN absorption lines with very high signal-to-noise ratio were observed recently by Ritchey, Federman & Lambert (2011) along 13 lines of sight through diffuse molecular clouds. Their careful analysis of the CN rotational excitation implies a mean excess over the temperature of the CMB of only 29 ± 3 mK, which is significantly lower than previous measurements. If electron impact is the dominant local CN excitation process, as it is generally assumed, then the excess temperature can yield an estimate of the electron density in the gas (Black & van Dishoeck 1991). The electron density is a crucial parameter for modelling both the physics and chemistry of molecular clouds. It is generally estimated from the observation of ultraviolet lines of atomic species like C and C^+. In clouds of modest density ($n(H_2) \lesssim 1000\,\mathrm{cm}^{-3}$) the fractional ionization ($x_e = n(e)/n(H_2)$) is thus typically 10^{-5}–10^{-4}. An accurate and independent determination of the electron density from CN excitation obviously requires a good knowledge of the electron-impact excitation rate coefficients.

The first cross-section calculations for the electron-impact rotational excitation of CN were based on the Born approximation (Thaddeus & Clauser 1966). More accurate close-coupling calculations were then performed (Allison & Dalgarno 1971) and these were found to agree with the Born results (for the $N = 0 \rightarrow 1$ transition) within a factor of 3 above ∼15 K (Thaddeus 1972). More recently, we have revisited the rotational excitation of the CN radical using the R-matrix approach combined with the infinite-order-sudden (IOS) approximation to derive, for the first time, electron-impact spin-coupled cross-sections (Harrison, Tennyson & Faure 2012). Our calculations were restricted to electron energies above 0.1 eV and the high energy results were found to be heavily influenced by both the A $^2\Pi$ and B $^2\Sigma^+$ excitation thresholds at 1.52 and 3.49 eV, respectively. At energy below these thresholds, however, the usual propensity rule for parity-conserving transitions ($\Delta j = \Delta N$) was found to hold.

⋆ E-mail: stephen.harrison@alumni.ucl.ac.uk

In this work, we extend the calculations of Harrison et al. (2012) to lower collision energies in order to derive rate coefficients down to the low temperatures of the interstellar medium. In addition to the spin-doubling of CN, we consider also the hyperfine structure. In Section 2, the method employed to derive the fine and hyperfine rate coefficients is outlined and comparisons with other sets of collisional data are presented. In Section 3, the results of radiative transfer calculations, including the CMB radiation and local excitation caused by electron and neutral collisions, are presented and compared to observational results. Conclusions are drawn in Section 4.

2 RATE COEFFICIENT CALCULATIONS

Electron-impact rate coefficients for both fine and hyperfine transitions were calculated from the pure rotational rate coefficients using the IOS formalism. The rotational cross-sections were computed as in Harrison et al. (2012) by combining R-matrix calculations (Tennyson 2010; Harrison & Tennyson 2012), Born corrected for dipolar transitions (Norcross & Padial 1982), with the adiabatic-nuclei-rotation (ANR) approximation, which is very similar to the IOS approximation. Both approximations consist of assuming that the target rotational states are degenerate, which is valid when the rotational spacings are negligible with respect to collisional energy. In practice, cross-sections were obtained for collision energies above 10 meV and they were corrected using a kinematic ratio to account for the rotational spacings, as in Harrison et al. (2012). They were finally extrapolated down to the rotational thresholds using the procedure described in Rabadan, Sarpal & Tennyson (1998), see equation 1 of their paper, which was calibrated using the rotational close-coupling results of Allison & Dalgarno (1971). Assuming that the electron velocity distribution is Maxwellian, rate coefficients were obtained for temperatures in the range 10–1000 K and for transitions among all levels up to $N = 20$. A similar study by Faure et al. (2007) considered hyperfine structure in electron collisions with the electron spin singlet HCN/HNC system which therefore does not display fine structure splitting.

Within the ANR or IOS formalism, the spin-coupled or fine structure rate coefficients (and cross-sections) can be obtained from the fundamental pure rotational cross-sections, i.e. those out of the lowest $N = 0$ level, as follows (see Harrison et al. 2012 and references therein):

$$k^{\rm IOS}_{Nj\rightarrow N'j'}(T) = (2N+1)(2N'+1)(2j'+1)\sum_{\lambda} \times \begin{pmatrix} N' & N & \lambda \\ 0 & 0 & 0 \end{pmatrix}^2 \begin{Bmatrix} \lambda & j & j' \\ S & N' & N \end{Bmatrix}^2 \times k_{0\rightarrow\lambda}(T), \quad (1)$$

where N is the rotational angular momentum of CN, S is the electron spin (here S =1/2), $\boldsymbol{j} = \boldsymbol{N} + \boldsymbol{S}$ and $k_{0\rightarrow\lambda}(T)$ is the pure rotational rate coefficients out of the lowest $N = 0$ level. In practice, as the rotational cross-sections were corrected for threshold effects and extrapolated, equation (1) is expected to be accurate only above $T \sim 100$ K. We have therefore implemented the 'scaling' method originally proposed by Neufeld & Green (1994) in which the spin-coupled rate coefficients are obtained as

$$k_{Nj\rightarrow N'j'}(T) = \frac{k^{\rm IOS}_{Nj\rightarrow N'j'}(T)}{k^{\rm IOS}_{N\rightarrow N'}(T)} k_{N\rightarrow N'}(T), \quad (2)$$

where

$$k^{\rm IOS}_{N\rightarrow N'}(T) = (2N'+1)\sum_{\lambda} \begin{pmatrix} N' & N & \lambda \\ 0 & 0 & 0 \end{pmatrix}^2 k_{0\rightarrow\lambda}(T). \quad (3)$$

The scaling of equation (2) guarantees in particular the following equality:

$$\sum_{j'} k_{Nj\rightarrow N'j'}(T) = k_{N\rightarrow N'}(T). \quad (4)$$

We also note that in equations (1) and (3) the fundamental excitation rates $k_{0\rightarrow\lambda}$ were replaced by the corresponding de-excitation rates using the detailed balance relation, as suggested by Faure & Lique (2012):

$$k_{0\rightarrow\lambda}(T) = (2\lambda+1)k_{\lambda\rightarrow 0}(T). \quad (5)$$

Similarly, the rate coefficients among hyperfine structure levels (N, j, F) can be obtained from the fundamental spin-coupled rate coefficients $k_{0,\,1/2\rightarrow L,\,L+1/2}(T)$ using the following formula (Faure & Lique 2012)

$$k^{\rm IOS}_{NjF\rightarrow N'j'F'}(T) = (2j+1)(2j'+1)(2F'+1)\sum_{\lambda} \frac{2\lambda+1}{\lambda+1} \times \begin{pmatrix} j' & \lambda & j \\ -1/2 & 0 & 1/2 \end{pmatrix}^2 \begin{Bmatrix} j & j' & \lambda \\ F' & F & I \end{Bmatrix}^2 \times \frac{1}{2}[1-\epsilon(-1)^{j+j'+L}]k_{0,1/2\rightarrow L,L+1/2}(T), \quad (6)$$

where ϵ is equal to $+1$ if the parity of initial and final rotational Nj level is the same or -1 if the parity of initial and final rotational Nj level differ. As above, a similar scaling was implemented:

$$k_{NjF\rightarrow N'j'F'}(T) = \frac{k^{\rm IOS}_{NjF\rightarrow N'j'F'}(T)}{k^{\rm IOS}_{Nj\rightarrow Nj'}(T)} k_{Nj\rightarrow Nj'}(T), \quad (7)$$

where

$$k^{\rm IOS}_{Nj\rightarrow N'j'}(T) = (2j'+1)\sum_{\lambda} \frac{2\lambda+1}{\lambda+1} \begin{pmatrix} j' & \lambda & j \\ -1/2 & 0 & 1/2 \end{pmatrix}^2 \times \frac{1}{2}[1-\epsilon(-1)^{j+j'+\lambda}]k^{\rm IOS}_{0,1/2\rightarrow\lambda,\lambda+1/2}(T). \quad (8)$$

Finally, the fundamental excitation rates $k_{0,\,1/2\rightarrow\lambda,\,\lambda+1/2}$ were replaced by the corresponding de-excitation rates using detailed balance.

Full details on the above procedure can be found in Faure & Lique (2012), where scaled IOS rate coefficients are compared in detail with almost exact recoupling calculations on CN–H_2. The scaled IOS method was found by these authors to reproduce the recoupling results within a factor of 3 or better, down to very low temperature. Results should be even better for electron collisions since the electron motion is much more rapid than H_2 and the adiabatic rotational approximation holds at lower temperature. It should be emphasized that the IOS method properly includes the recoupling algebra, via the 3-j and 6-j coefficients, and the propensity rules $\Delta j = \Delta N$ (parity conserving) and $\Delta j = \Delta F$ are correctly predicted. Faure & Lique (2012) showed that these rules play an important role in radiative transfer applications when line saturation is important.

Figs 1 and 2 present the rotational rates $0 \rightarrow 1$ and $0 \rightarrow 2$ as a function of temperature, up to 1000 K, including a comparison with the relevant data from the work of Allison & Dalgarno (1971) which has been so far employed in the astronomical literature. It is clear

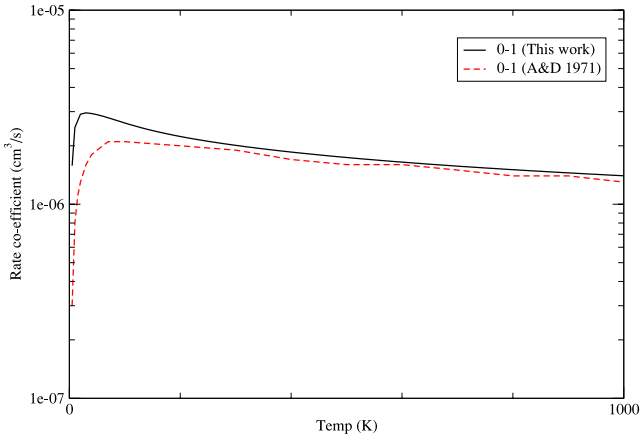

Figure 1. A comparison of the $0 \rightarrow 1$ rotational rate of this work with the rate of Allison & Dalgarno (1971).

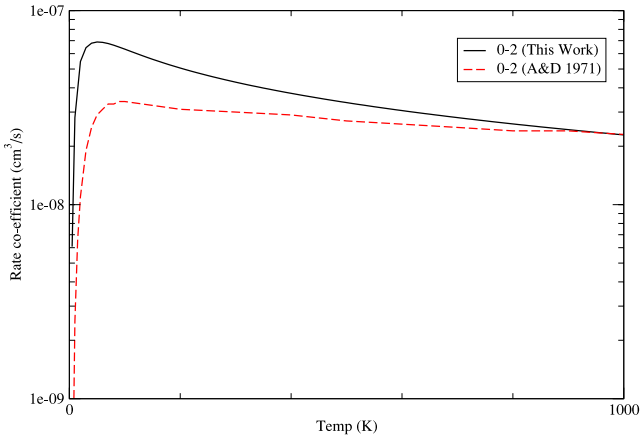

Figure 2. A comparison of the $0 \rightarrow 2$ rotational rate of this work with the rate of Allison & Dalgarno (1971).

that the present rotational rates are larger than those of Allison & Dalgarno (1971), particularly at temperatures below 100 K where our data are about a factor of 2 larger at the peaks. These differences reflect both the short-range treatment of the interaction and the extrapolation at very low energy.

Fig. 3 shows the fine structure e-CN collision rates out of the $N = 5$, $j = 5.5$ initial level in comparison with the relevant data from the work of Kalugina, Lique & Klos (2012) for CN colliding with para-$H_2(j = 0)$. We can notice that dipolar transitions with $\Delta N = 1$ have the largest rates for e-CN, in contrast to CN–$H_2(j = 0)$ collisions where transitions with $\Delta N = 2$ are preferred. We note, however, that dipolar transitions are also favoured in the case of CN colliding with rotationally excited H_2 ($j > 0$) (Lique, private communication). For both systems, the propensity rule $\Delta j = \Delta N$ (i.e. parity-conserving transitions) is observed. As a result, the favoured transitions are $(N, J) = (5, 5.5) \rightarrow (4, 4.5)$ and $(5, 5.5) \rightarrow (3, 3.5)$ for electron and $H_2(j = 0)$ collisions, respectively, and they differ by about four orders of magnitude. Finally, we note that the temperature dependences are very weak (for these de-excitation transition) in the 10–100 K range.

Figs 4–6 also give the hyperfine structure rate comparisons between this work and Kalugina et al. (2012) for the transitions out of the $N = 2$, $j = 2.5$, $F = (1.5–3.5)$ respectively. As expected, the highest electron-impact rate is observed for the dipolar transitions $(2, 2.5, 2.5) \rightarrow (1, 1.5, 1.5)$ and $(2, 2.5, 3.5) \rightarrow (1, 1.5, 2.5)$ corresponding to $\Delta N = \Delta j = \Delta F = 1$. These rates are about five orders of magnitude larger than the corresponding rates for $H_2(j = 0)$. For other transitions, the differences range between two and five orders of magnitude.

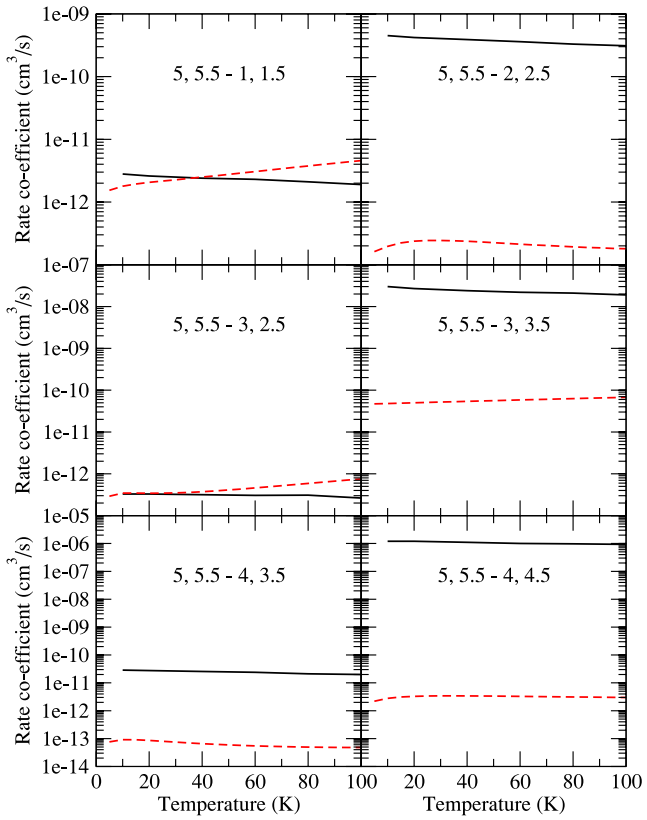

Figure 3. A comparison of the fine structure rate from the $(N, j) = (5, 5.5)$ initial level between this work (solid line) and the rate of Kalugina et al. (2012) (dashed line).

We conclude that the electron-impact excitation of CN should be significant as soon as the electron fraction $x_e = n(\mathrm{e})/n(H_2)$ exceeds $\sim 10^{-5}$ and that these collisions will strongly favour transitions with $\Delta N = \Delta j = \Delta F = 1$, in contrast to $H_2(j = 0)$ collisions which favour $\Delta N = \Delta j = \Delta F = 2$. The present data will be made available in the BASECOL data base (Dubernet et al. 2013).

3 RADIATIVE TRANSFER CALCULATIONS

As explained in Section 1, in diffuse molecular clouds the rotational excitation of CN is controlled by a competition between the collisional excitation and the interaction with the CMB radiation. This competition results in an excess of the CN rotational excitation over the temperature of the CMB (2.725 K). The CN excitation temperature, determined from optical absorption lines, is thus defined as

$$T_{\mathrm{ex}}(\mathrm{CN}) = T_{\mathrm{CMB}} + T_{\mathrm{loc}}, \tag{9}$$

where T_{loc} is the contribution due to local excitation mechanism and T_{ex} is determined through the Boltzmann equation:

$$\frac{N(i)}{N(j)} = \frac{g_i}{g_j} \exp\left(-\frac{h\nu_{ij}}{k_B T_{\mathrm{ex}}}\right), \tag{10}$$

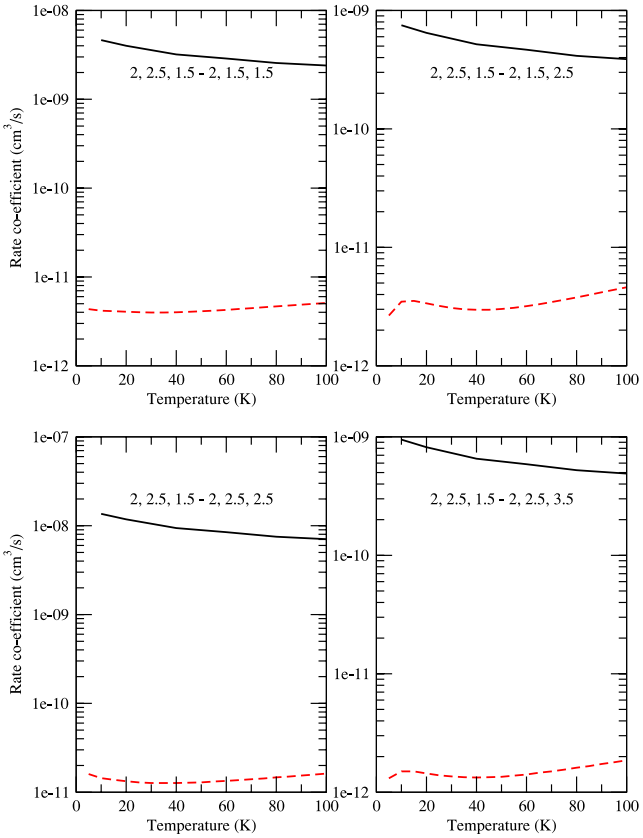

Figure 4. A comparison of the hyperfine structure rate from the (N, J, F) = (2, 2.5, 1.5) initial level between this work (solid line) and the rate of Kalugina et al. (2012) (dashed line).

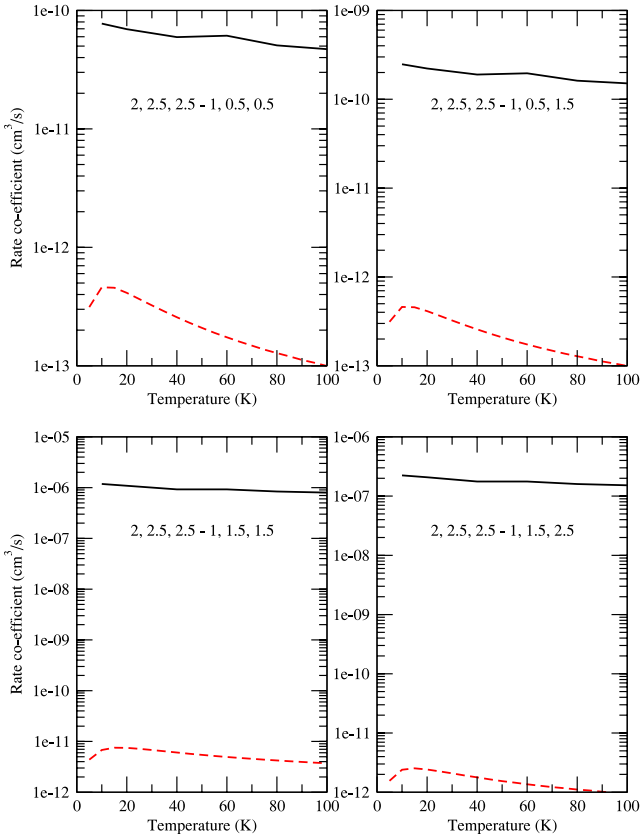

Figure 5. A comparison of the hyperfine structure rate from the (N, J, F) = (2, 2.5, 2.5) initial level between this work (solid line) and the rate of Kalugina et al. (2012) (dashed line).

where $N(i)$ and $N(j)$ are the column densities of the upper and lower rotational states, respectively, and $g(i)$ and $g(j)$ are the corresponding statistical weights. In practice, only the three lowest rotational states are significantly populated, i.e. $N = 0$, 1 and 2, yielding the measured excitation temperatures T_{01}(CN) and T_{12}(CN). The local excitation effects can be also directly determined from a measurement of CN millimetre emission which is unfortunately weak and rarely detected.

Observationally, the most recent CN optical absorption-line measurements have provided a weighted mean value of $T_{01}(\mathrm{CN}) = 2.754 \pm 0.002$ K, implying an excess over the temperature of the CMB of $T_{\mathrm{loc}} = 29 \pm 3$ mK (Ritchey et al. 2011). We note that the dispersion of these measurements is quite large, i.e. 134 mK, with some sight lines showing (unphysical) excitation temperature below T_{CMB}. It is generally assumed that electron-impact excitation is the dominant contribution to this excess temperature. Below we investigate the influence of varying the electron density on the local excitation, using a radiative transfer code combined with the best available electron and neutral collisional rates: those from this work for electrons and those of Kalugina et al. (2012) for para-H_2($j = 0$), assumed to be identical for hydrogen atoms.[1] This kind of analysis has been previously performed by Black & van Dishoeck (1991) with old collision data.

Radiative transfer calculations were performed with the RADEX code (van der Tak et al. 2007), using the Large Velocity Gradient approximation for an expanding sphere. The kinetic temperature was fixed at $T = 20$ K, as in the calculations of Ritchey et al. (2011). The line width (full width at half-maximum) was taken to be 1.0 kms^{-1}, corresponding to a Doppler line broadening parameter b of 0.6 kms^{-1}. The column density was taken at two typical values $N(\mathrm{CN}) = 3 \times 10^{12}$ and 3×10^{13} cm^{-2}. The density of neutral collision partners ($n = n(\mathrm{H}) + n(\mathrm{H_2})$) was fixed at three representative values: 100, 300 and 1000 cm^{-3}. Finally, the electron abundance was varied from 2×10^{-3} to 1 cm^{-3}, corresponding to electron fractions $n(e)/n$ in the range 2×10^{-6} to 10^{-2}. Results are presented in Fig. 7. In each panel, the excitation temperature T_{01}(CN) is plotted as a function of the electron abundance. It should be noted that our excitation calculations provide the populations of hyperfine levels, from which T_{01} was computed by summing over hyperfine sublevels. The dashed horizontal line gives the CMB at 2.725 K while the horizontal dotted line gives the measured excitation temperature T_{01} at 2.754 K. We first observe that the excess temperature of 29 mK cannot be reproduced at very low electron density, indicating that neutral collisions alone cannot explain the local excitation of CN. This confirms the conclusions of past investigators (Thaddeus 1972; Black & van Dishoeck 1991). Secondly, it can be noticed that the local excitation is reproduced for a rather restricted range of electron densities: from 0.01 cm^{-3} at $n = 1000$ cm^{-3} to 0.06 cm^{-3} at $n = 100$ cm^{-3} with a weak dependence on the CN column density. Assuming that hydrogen is entirely molecular, these electron

[1] We note that the rate coefficients for ortho-H_2($j = 1$) exceed those for para-H_2($j = 0$) by up to a factor of 10 (Lique, private communication). However, ortho-H_2($j = 1$) can be neglected here since its abundance in cold ($T < 30$ K) diffuse clouds is expected to be at least 30 times lower than that of para-H_2($j = 0$).

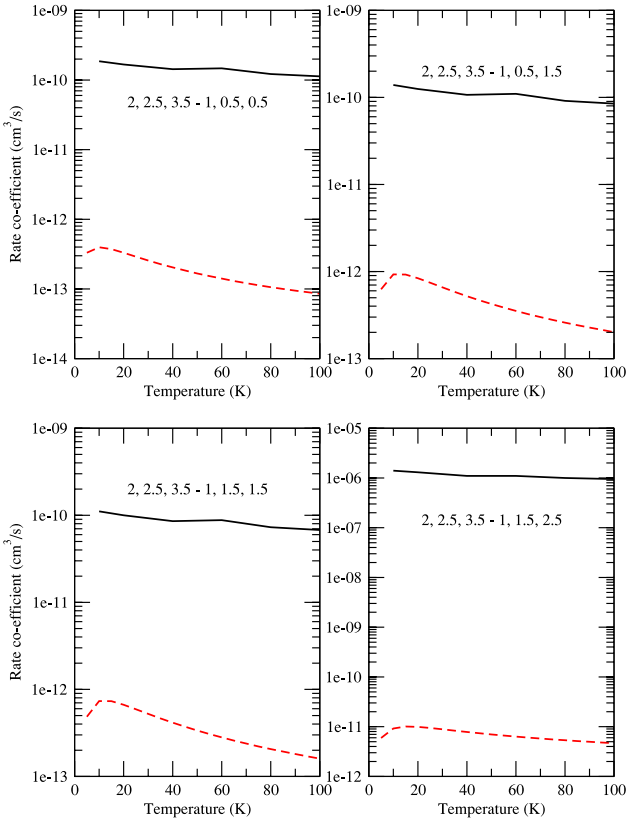

Figure 6. A comparison of the hyperfine structure rate from the (N, J, F) = (2, 2.5, 3.5) initial level between this work (solid line) and the rate of Kalugina et al. (2012) (dashed line).

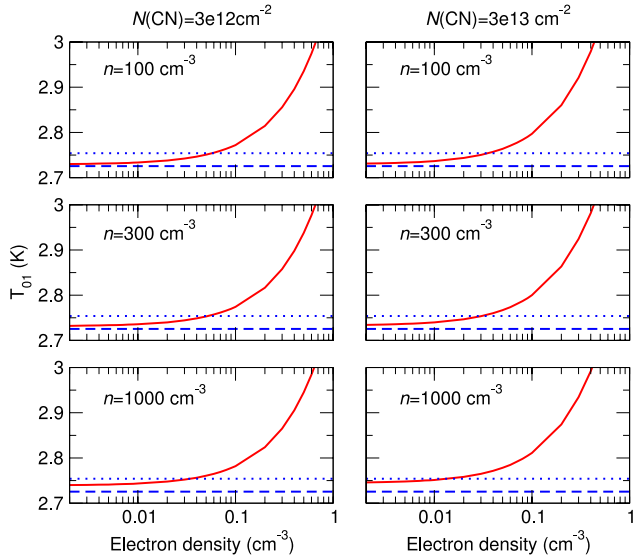

Figure 7. Excitation temperature T_{01}(CN) as a function of electron density for different densities ($n = n_{\rm H} + n_{\rm H_2}$) and CN column densities, at a single kinetic temperature of 20 K. Here the dashed line represents the CMB at 2.725 K while the dotted blue line gives the measured average excitation temperature at 2.754 K (Ritchey et al. 2011).

densities correspond to electron fractions ($x_e = n(e)/n(\rm H_2)$) in the range 10^{-5}–6×10^{-4}. This is consistent with the abundance of interstellar C^+ ($n(C^+)/n(\rm H_2) \sim 3 \times 10^{-4}$) which is the main source of electrons in the diffuse interstellar medium.

In fact, more accurate determination of the electron density can be achieved for clouds where the physical conditions are reasonably well known. For instance, the kinetic temperature and the collision density were determined for the source HD 154368 from the analysis of C_2 excitation by Sonnentrucker et al. (2007). These authors found $T = 20 \pm 5$ K and $n = 150^{+50}_{-25}$, with n(H) = 60 cm^{-3} and $n(\rm H_2)$ = 90 cm^{-3}. The CN column density towards the star HD 154368 is 2.7×10^{13} cm^{-2} and the line width is 1.2 kms^{-1} (Ritchey et al. 2011). Interestingly, this source also shows the second highest excitation temperature T_{01}(CN) = 2.911±0.004 K, which is significantly larger than the weighted mean value of 2.754 K. Using the physical conditions determined by Sonnentrucker et al. (2007), we have found that an electron density of 0.3 cm^{-3} is necessary to reproduce the measured T_{01} towards HD 154368. This corresponds to an electron fraction $n(e)/n(\rm H_2) \sim 3 \times 10^{-3}$, which is too high with respect to the available carbon. Ritchey et al. (2011) obtained an even larger value of 0.69 cm^{-3} for HD 154368 and concluded that it probably corresponds to an upper limit considering the dispersion of 134 mK. In fact, for this source, Palazzi et al. (1990) have detected a weak emission of CN: the strongest hyperfine component (N, J, F) = (1, 1.5, 2.5) → (0, 0.5, 1.5) at 113.49 GHz with an antenna temperature $T_R^* = 19 \pm 5.1$ mK. Fig. 8 shows that this value (blue hatched zone) is reproduced for an electron density of $\sim 3 \times 10^{-2}$ cm^{-3}, corresponding to an electron fraction $n(e)/n(\rm H_2) \sim 3 \times 10^{-4}$, as expected if carbon is fully ionized. In addition, the corresponding excitation temperature is T_{01} = 2.75 K, in very good agreement with the weighted mean value of 2.754 K determined by Ritchey et al. (2011).

In summary, our calculations suggest that in the diffuse cloud regions where CN resides, the electron density lie in the range $n(e) \sim 0.01$–0.06 cm^{-3}. This range is significantly smaller than that derived by Black & van Dishoeck (1991), $n(e) \sim 0.02$–0.5 cm^{-3}, reflecting the low (mean) excess temperature $T_{\rm loc} = 29 \pm 3$ mK derived by Ritchey et al. (2011). On the other hand, for individual sources, we have shown that the dispersion of the optical measurements (∼134 mK) must be taken into account, as recommended by Ritchey et al. (2011). In fact, the weak millimetre emission of CN probably provides the best accurate measurement of $T_{\rm loc}$, which in

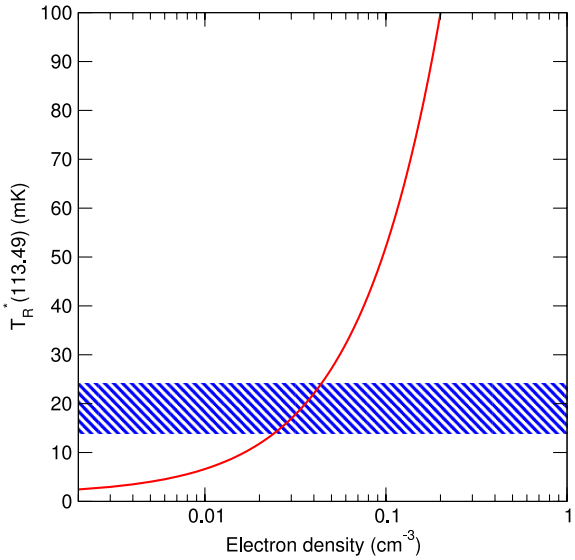

Figure 8. Plot of the intensity of the line at 113.49 GHz as a function of electron density for $T = 20$ K, $n = 150$ cm^{-3} and N(CN) = 2.7×10^{13} cm^{-2}. Here the blue hatched zone shows the observed antenna temperature.

turn yields an accurate determination of $n(e)$ if the kinetic temperature and hydrogen density are known. Thus, the electron density $n(e) \sim 3 \times 10^{-2}\,\mathrm{cm}^{-2}$ derived for HD 154368 might represent the best indirect measurement of electron density in a diffuse cloud.

4 CONCLUSIONS

In this work, we present a comprehensive set of rates for fine-structure and hyperfine-structure resolved electron-impact rotational excitation of the CN radical. Similar rates have previously been used in an attempt to determine electron densities from shocked regions of the interstellar medium (Jimenez-Serra et al. 2006; Roberts et al. 2010). Here we consider the observed temperature excess of CN in diffuse clouds over the CMB. Assuming that this excess is due to electron and neutral collisions, with electron impact being predominant, our calculations suggest that the electron density lies in the range $n(e) \sim 0.01$–$0.06\,\mathrm{cm}^{-3}$ for typical physical conditions present in diffuse clouds. This range of values is consistent with the known abundance of carbon which is thought to be the main source of free electrons. We suggest that our methodology provides a viable means of determining electron densities in the diffuse interstellar medium.

ACKNOWLEDGEMENTS

We thank François Lique for useful discussions. This work has been supported by STFC through a studentship to SH and the French CNRS national programme 'Physique et Chimie du Milieu Interstellaire' (PCMI).

REFERENCES

Allison A. C., Dalgarno A., 1971, A&A, 13, 331
Black J. H., van Dishoeck E. F., 1991, ApJ, 369, L9
Dubernet M.-L. et al., 2013, A&A, 553, A50
Faure A., Lique F., 2012, MNRAS, 425, 740
Faure A., Varambhia H. N., Stoecklin T., Tennyson J., 2007, MNRAS, 382, 840
Field G. B., Hitchcock J. L., 1966, ApJ, 146, 1
Fixsen D. J., 2009, ApJ, 707, 916
Harrison S., Tennyson J., 2012, J. Phys. B: At. Mol. Opt. Phys., 45, 035204
Harrison S., Tennyson J., Faure A., 2012, J. Phys. B: At. Mol. Opt. Phys., 45, 175202
Jimenez-Serra I., Martin-Pintado J., Viti S., Martin S., Rodriguez-Franco A., Faure A., Tennyson J., 2006, ApJ, 650, L135
Kalugina Y., Lique F., Klos J., 2012, MNRAS, 422, 812
Leach S., 2012, MNRAS, 421, 1325
Mather J. C., 1990, ApJ, 354, L37
Neufeld D. A., Green S., 1994, ApJ, 432, 158
Norcross D. W., Padial N. T., 1982, Phys. Rev. A, 25, 226
Palazzi E., Mandolesi N., Crane P., Kutner M. L., Blades J. C., Hegyi D. J., 1990, ApJ, 357, 14
Penzias A. A., Wilson R. W., 1965, ApJ, 142, 419
Rabadan I., Sarpal B. K., Tennyson J., 1998, MNRAS, 299, 171
Ritchey A. M., Federman S. R., Lambert D. L., 2011, ApJ, 728, 36
Roberts J. F., Jimenez-Serra I., Martin-Pintado J., Viti S., Rodriguez-Franco A., Faure A., Tennyson J., 2010, A&A, 513, A64
Sonnentrucker P., Welty D. E., Thorburn J. A., York D. G., 2007, ApJS, 168, 58
Tennyson J., 2010, Phys. Rep., 491, 29
Thaddeus P., 1972, ARA&A, 10, 305
Thaddeus P., Clauser J. F., 1966, Phys. Rev. Lett., 16, 819
van der Tak F. F. S., Black J. H., Schöier F. L., Jansen D. J., van Dishoeck E. F., 2007, A&A, 468, 627

This paper has been typeset from a TEX/LATEX file prepared by the author.